

Article

# Assessment of Meteorological Drought and Wet Conditions Using Two Drought Indices Across KwaZulu-Natal Province, South Africa

Minenhle Siphesihle Ndlovu <sup>1,2</sup> and Molla Demlie <sup>1,\*</sup> 

<sup>1</sup> School of Agricultural, Earth and Environmental Sciences, University of KwaZulu-Natal, Westville Campus, Private Bag 54001, Durban 4000, South Africa; ndlovusiphesihle70@gmail.com

<sup>2</sup> GCS Water and Environmental Consultants, 4a old Main Road, Judges Walk, Kloof, KwaZulu-Natal 3610, South Africa

\* Correspondence: demliem@ukzn.ac.za

Received: 7 April 2020; Accepted: 22 May 2020; Published: 12 June 2020



**Abstract:** South Africa has been experiencing a series of droughts for the last few years, limiting the availability of water supply in reservoirs and impacting many sectors of the economy. These droughts have affected even the wetter eastern provinces including KwaZulu-Natal. This paper presents the results of analyses and assessment of meteorological drought across KwaZulu-Natal (KZN) Province of South Africa using two drought indices. The main objective of the study is to understand the changes in rainfall patterns for a period of 48 years (i.e., 1970 to 2017) and identify wet and dry years. The percent of normal precipitation index (PNPI) and rainfall anomaly index (RAI) were used to explore and categorize the wet and dry periods at 18 selected rainfall gauging stations across the province. Mann–Kendall statistics and Sen’s slope were employed on the indices to further understand the trend of drought conditions. The results revealed that 1992 and 2014/15 were the most extremely dry years with 2015 being the driest year over the studied period induced by El Niño. The extremely wet periods were 1987, 1996, and 2000 which have been associated with cyclonic events. Droughts have become more frequent and intense, while wet conditions are less frequent. The drought condition was observed not to be peculiar to one region and to vary from year-to-year. These variations have been associated with global climate drivers including El Niño-southern oscillation (ENSO) and sea surface temperature (SST) conditions. The northern region around Magudu, Hlobane, Vryheid and Dundee were relatively the most affected during periods of extreme drought conditions. Comparative analysis showed that RAI is more robust than PNPI in understanding drought conditions. Thus, it can be applied effectively in Southern Africa in analyzing dry and wet conditions.

**Keywords:** drought indices; ENSO; meteorological drought; rainfall anomaly index; KwaZulu-Natal; percent of normal precipitation index; South Africa

## 1. Introduction

South Africa is a semi-arid country characterized by spatial and temporal variability of rainfall [1] and is considered a water-stressed country. Its average annual rainfall is less than 500 mm/year, which is below the world average of about 860 mm/year. In recent decades, the rainfall of the region has become unpredictable and extremes in the form of droughts and floods are not uncommon. Drought is the most complex natural hazard and is often defined as the temporary meteorological event that stems from the shortage of precipitation over an extended period of time compared to a long term average condition [2]. The Department of Water and sanitation [3,4] reported that the 2015 rainfall across the country was below normal. These extreme conditions that caused severe summer drought

and rainfall variability in South Africa tend to occur due to regional processes such as El Niño and sea surface temperature (SST) conditions. The El Niño-southern oscillation (ENSO) is known to influence rainfall in most parts of the southern African regions with the negative phase being associated with drought conditions and the positive phase associated with above average rainfall [5–8]. This is characterized by low pressure anomalies coupled with cyclonic circulation [9]. Sea surface temperature variations in the Indian Ocean influence the atmospheric dynamics and moisture supply over Southern Africa [10–13]. According to [14] the Indian Ocean SST anomalies could shift atmospheric convection and rainfall eastwards during El Niño events. Based on climate projections, [15] reported that the most severe drought impacts are likely to occur in the western part of South Africa, where small towns and subsistence farmers are more vulnerable. For instance, in 2017 the Western Cape Province of South Africa experienced the worst water shortage in 113 years and was declared by the government as a disaster region [16]. Drought generally affects wider areas and more people than any other natural disaster [17–19] and has considerable impacts on the various sectors of the economy including agriculture. The consequences of which depends on social vulnerability at the time in which the drought occurs [20].

Wilhite, D.A. et al. in [21,22] classified drought into four types, namely, meteorological, hydrological, agricultural and socio-economic droughts. Meteorological drought occurs when precipitation is less than normal and is characterized by changes in weather patterns. Increased temperature, evapotranspiration and solar radiation, and decrease in humidity and cloudiness are the first indicators of drought occurrence [2,19].

Various approaches have been followed to study drought. One of these methods is using drought indices (DI) as they explain the cumulative effects of a prolonged and abnormal moisture deficiency [23,24]. Numerous indices have been developed for studying drought, while none has inherent priority over others, some have better performance in specific conditions [20].

The most extensively used drought indices for water resource management, monitoring, and drought prediction include, but are not limited to Palmer drought severity index [25], surface water supply index [26], standardized precipitation index (SPI) [27], percentage of normal precipitation index (PNPI) [28], rainfall anomaly index (RAI) [29] and crop specific drought index [30]. The SPI is based on the probability of rainfall for any time scale (yearly, seasonally, and monthly) and its calculation is dependent on the distribution of rainfall over longer periods of time of more than 50 years [27]. The PNPI is the rainfall average calculated over at least a 30-year period [28]. The number of years described above are recommendations on having enough data and thus are not requirements in the calculations of drought indices. The RAI, developed by [29], is another index for studying drought severity and is based on the calculated precipitation against random values [31] and have been applied in various studies. The Mann–Kendall trend test and Sen’s slope have been used successfully in analysis the statistical variation, distribution and frequency of drought indices [32,33]. The aim of this paper is to characterize and understand the changes in rainfall patterns, frequency, severity, spatial and temporal distribution of meteorological drought and wet conditions across the KZN province of South Africa using PNPI and RAI drought indices. In light of the recurrent dry spells across Southern Africa in general and South Africa in particular, analyses and assessment of meteorological drought is critical in making informed decisions for better management of the ever-meager water resources and to proactively develop future water supply and allocation strategies.

## 2. Description of the Study Area

### 2.1. Location and Physiography

KZN province is located in eastern South Africa and shares borders with Eastern Cape, Free State and Mpumalanga provinces as well as the kingdoms of Lesotho, Swaziland and the state of Mozambique (Figure 1). According to Statistics South Africa [34], KZN has a population of about 10.3 million and a surface area of about 93,350 km<sup>2</sup>. The topography of the province varies from the interior to the

coast (Figure 1). The altitude ranges from 3448 m above mean sea level (amsl) along the Drakensberg escarpment in the west to low mountains in the midlands, highly dissected, undulating hills and drops to sea level at the coast.

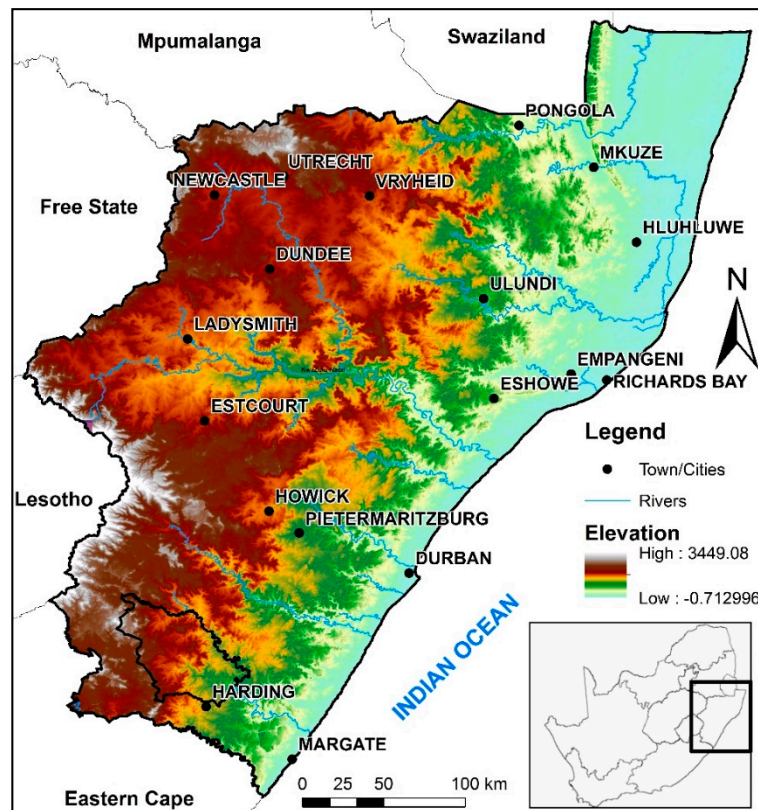


**Figure 1.** Location map of the study area along with digital elevation model indicating variations in topography (elevation data from [35]).

## 2.2. Climate and Regional Moisture Sources

KZN has a subtropical climate, where dry and cold winter occurs from April to August and hot and humid summer occurs from September to March which is the main rainy season. In summer, mean temperatures often rise above 25 °C and in winter, the mean temperature drops to an average of about 20 °C. Coastal areas around Richards Bay and Durban receive mean annual precipitation (MAP) of about 1193 and 964 mm/year, respectively. The midlands of KZN around Pietermaritzburg and the north-western part of the province, around Newcastle, receive a MAP of about 813 mm/year and 847 mm/year, respectively. While the south-eastern coastal areas, around Margate receive 1382 mm/year. The wide variability of climatic conditions in the province is a result of the large variation in physiographic features. The province's rainfall is controlled by the position of South Indian Ocean ENSO and SST. The main source of moisture to the region is the South-western Indian Ocean, the western tropical Indian Ocean north of Madagascar [36] and east of Madagascar, the Agulhas gyre and local forcing and feedback mechanisms [15].

## 3. Methodology and Data

### 3.1. Precipitation Data

Rainfall data used for this study was sourced from the South African Weather Service and data gaps were filled according to standard procedures of the normal ratio method [37,38]. Nineteen (19) rainfall stations located across KZN province (Figure 2) were used for studying general precipitation characteristics and analyzing trends in drought conditions for the period from 1970 to 2017. The mean

annual rainfall information for each weather station and corresponding data record period considered in the study are summarized in Table 1.

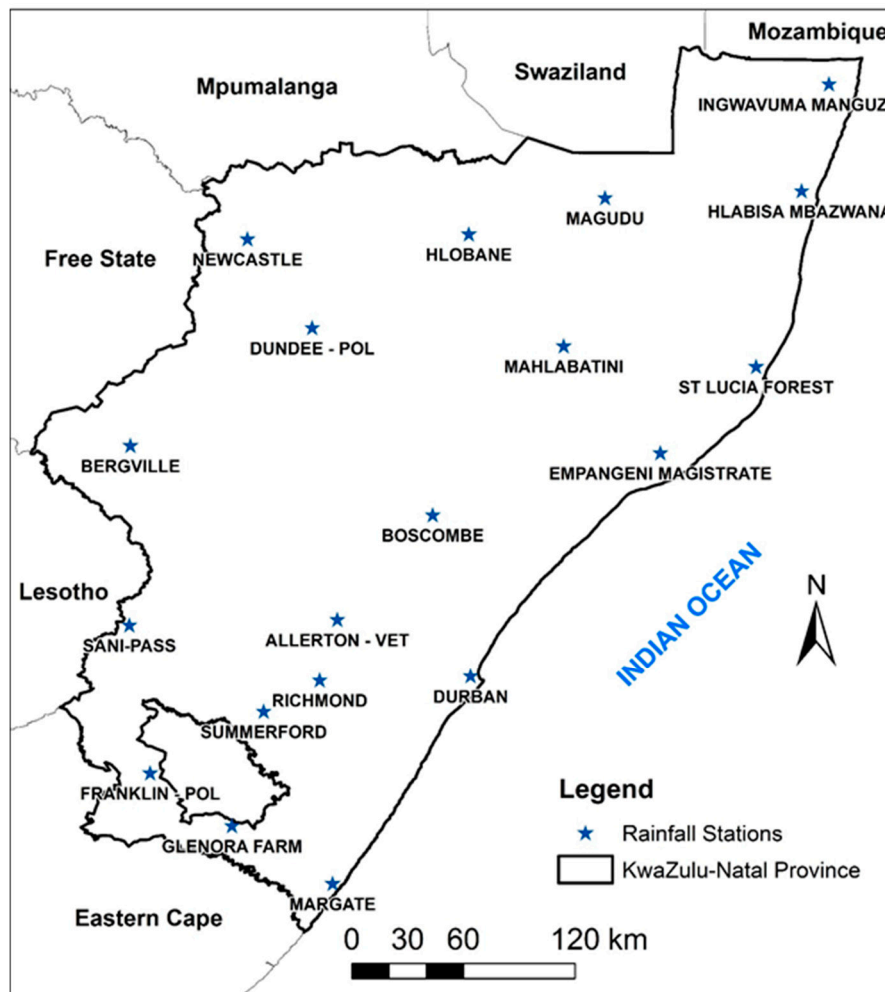


Figure 2. Spatial distribution of the weather stations in KZN analyzed in this study.

Table 1. Mean annual rainfall and record period used at each weather station.

Station	Location		Altitude (m amsl)	Record Period	Mean Rainfall (mm)
	Lat	Long			
Ingwavuma-Manguzi	-26.9830	32.7329	69	1987–2017	827.9
Hlabisa- Mbazwana	-27.5000	32.6000	55	1970–2017	839.1
Hlobane	-27.7089	30.9914	1294	1970–2017	860.6
Newcastle	-27.7322	29.9211	1241	1984–2017	846.7
Dundee	-28.1619	30.2339	1256	1970–2017	720.8
Mahlabathini	-28.2500	31.4500	757	1970–2017	788.3
St.Lucia Forest	-28.3500	32.3800	44	1970–2017	1168.3
Empangeni Magistrate	-28.7670	31.9170	74	1970–2017	997.5
Bergville	-28.7319	29.3550	1145	1970–2017	775.1
Boscombe	-29.0670	30.8170	1151	1970–2017	965.4
Sani-Pass	-29.6000	29.3500	2063	1970–2017	1049.2
Allerton Vet	-29.5736	30.3556	711	1970–2017	963.9
Richmond	-29.8700	30.2700	864	1970–2017	947.8
Durban	-29.8500	31.0000	76	1970–2017	964.2
SummerFord	-30.0208	29.9994	1233	1970–2017	871.9
Franklin Pol	-30.3175	29.4508	1532	1970–2017	711.6
Glenora Farm	-30.5714	29.8458	872	1970–2017	824.7
Margate	-30.8500	30.3330	127	1984–2017	1381.8

The plot of mean annual precipitation versus the altitude of the rainfall stations (Figure 3) does not show any conspicuous trend.

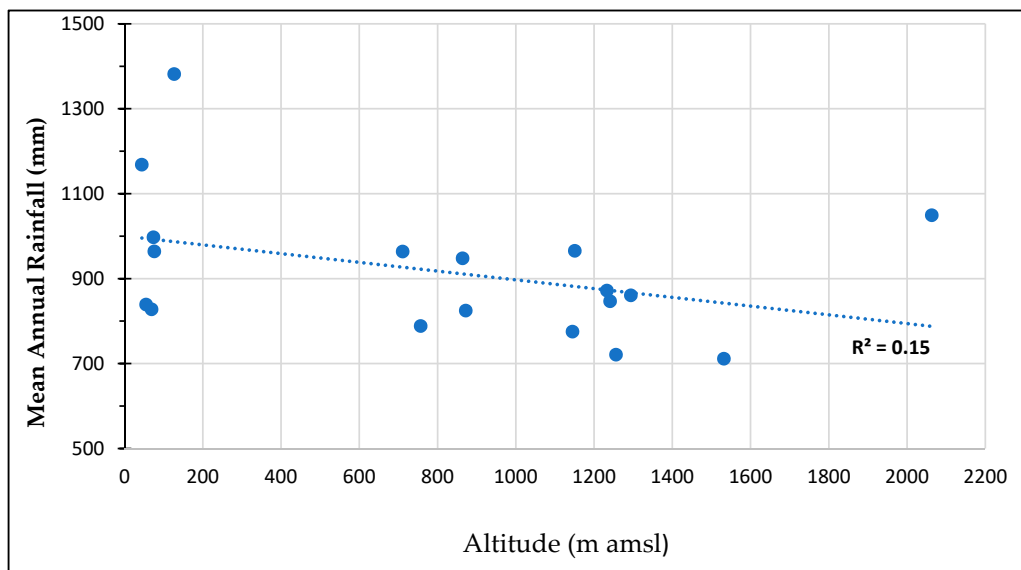


Figure 3. Rainfall-Altitude relationships for the rainfall stations considered in this study.

### 3.2. Drought Indices Used

A number of indices have been used for detecting and monitoring of meteorological, agricultural, hydrological and socio-economic droughts. In this study, two drought indices, namely the PNPI and RAI were used to study drought conditions across KZN province using long-term annual rainfall data.

#### Percentage of Normal Precipitation Index (PNPI):

The percent of normal precipitation index (PNPI) was developed by [29] and is based on the concept of dividing the actual precipitation by the normal precipitation. The PNPI index can be computed for a variety of time scales including a single month, group of months representing a particular season or annually. According to [39], this index yields the best results when used for a single region or a single season and is given by Equation (1) [29,39]:

$$PNPI = \frac{P_i}{P} \times 100, \tag{1}$$

where PNPI is the percentage of normal precipitation index,  $P_i$  is the actual precipitation for year  $i$  and  $P$  is the normal precipitation calculated over a 48-year period (from 1970 to 2017). The PNPI categories are grouped in terms of drought severity as indicated in Table 2.

Table 2. Percent of normal categories [40].

Category	Index (%)
Normal	>80
Weak drought	70–80
Moderate drought	50–70
Severe drought	40–50
Extreme drought	<40

#### Rainfall Anomaly Index (RAI):

RAI was developed by [29] and is considered the most effective and simple meteorological index. The RAI is calculated from precipitation data to analyze the intensity and frequency of the dry and wet

years [41]. This method can be applied in monthly or annual time scales and is given by Equations (2) and (3) [29]:

$$RAI = 3 \left[ \frac{P - \bar{P}}{\bar{m} - \bar{P}} \right] \text{ If } P > \bar{P}, \tag{2}$$

$$RAI = -3 \left[ \frac{P - \bar{P}}{\bar{X} - \bar{P}} \right] \text{ If } P < \bar{P} \tag{3}$$

where,  $\bar{P}$  is the long-term mean annual precipitation of the given rainfall station calculated over the whole data record period,  $P$  is the actual precipitation,  $\bar{m}$  is the average of the ten highest yearly precipitations in the historical record and  $\bar{X}$  is the average of the ten lowest yearly precipitations in the historical record. The drought index is then classified based on its severity as shown in Table 3.

**Table 3.** Classification of RAI drought severity (adapted from [29]).

Category	RAI
Extremely wet	$\geq 3.0$
Very Wet	2.0 to 2.99
Moderately wet	1.0 to 1.99
Slightly wet	0.50 to 0.99
Near Normal	0.49 to -0.49
Slightly dry	-0.50 to -0.99
Moderately dry	-1.0 to -1.99
Very dry	-2.0 to -2.99
Extremely dry	$\leq -3.00$

The spatial distributions of the drought indices across the studied province were mapped for each year by Kriging interpolation method using Surfer 15.0 software. The advantages of Kriging is that it accounts for directional influences and assumes that the distance between sample points reflect a spatial correlation that can be used to explain variation in the surface. The major disadvantage of the interpolation is the fact that it introduces some degree of uncertainty depending on the density of the interpolated points. However, since the interpolation helps in visualization of the spatiotemporal trend, it is preferable to the station-by-station description of the trend and magnitude of the changes in the drought indices.

### 3.3. Statistical Analyses

To understand the trends and the direction and magnitude of the change of the PNPI and RAI indices, statistical analyses were undertaken using the Mann–Kendall trend test and Sen’s slope.

#### Mann–Kendall Test

The Mann–Kendall test [41,42] is a non-parametric method commonly used for identifying and analyzing trends in time series hydrological data [32,43–45]. The major advantage of the Mann–Kendall test is that it is free from statistical distribution which is required in the parametric test. The null hypothesis ( $H_0$ ) in Mann–Kendal tests states that there is no trend or serial correlation between the analyzed population and the alternative hypothesis ( $H_1$ ) states existence of a trend assuming an increasing or decreasing trend. Data values are evaluated as an ordered time series where each data point is compared to all subsequent data values.

In the Mann–Kendall statistic,  $S$  is defined as [41,42]:

$$S = \sum_{i=1}^{n-1} \sum_{j=i+1}^n \text{sgn}(x_j - x_i), \tag{4}$$

where,  $sgn$  is the signum function. Application of the trend test is performed on a time series  $x_i$  ranked from  $i = 1, 2 \dots \dots n - 1$  and  $x_j$ , is ranked from  $j = i + 1, 2 \dots \dots n$ . Each data point  $x_i$  is used as a reference point and is compared with the test of data points  $x_j$  such that,

$$sgn(x_j - x_i) = \begin{cases} 1 \text{ if } (x_j - x_i) > 0 \\ 0 \text{ if } (x_j - x_i) = 0 \\ -1 \text{ if } (x_j - x_i) < 0 \end{cases} \quad (5)$$

where if  $n < 10$ , the value of  $S$  is compared directly to the theoretical value of  $S$  derived from Equation (4). At certain probability levels,  $H_0$  is rejected in favor of  $H_1$  if the absolute value of  $S$  equals or exceeds a specified value  $S_{\alpha/2}$ , where  $S_{\alpha/2}$  is the smallest  $S$  which has probability less than  $\alpha/2$  to appear in the case of no trend. A positive value of  $S$  indicates an upward trend and negative value indicates downward trend. The  $p$ -value for the Mann–Kendall test indicates the absence or presence of significant trends. If the computed value of  $p > p_{\alpha}$ , the null hypothesis ( $H_0$ ) is rejected at  $\alpha$  level of significance in a two-tailed test. For  $n \geq 10$ , Mann–Kendall statistics  $S$  is approximately normally distributed with variance ( $Var(s)$ ). The variance statistics is given by Equation (6) as:

$$Var(S) = \frac{n(n - 1)(2n + 5) + \sum t_i (t_i - 1)(2t_i + 5)}{18} \quad (6)$$

where,  $t_i$  is the number of ties present with  $i$  as extent. The presence of a statistically significant trend is evaluated using the standardized  $Z_c$  statistics Equation (7):

$$Z_c = \begin{cases} \frac{S-1}{\sqrt{Var(S)}} \text{ if } S > 0 \\ 0 \text{ if } S = 0 \\ \frac{S+1}{\sqrt{Var(S)}} \text{ if } S < 0 \end{cases} \quad (7)$$

where a positive value of  $Z_c$  indicates an increasing trend and a negative value indicates a decreasing trend. The standardized Mann–Kendall statistic  $Z_c$  follows the standard normal distribution. To test an increasing or decreasing trend of the drought indices, a two-tailed test at 5% level of significance is used.

**Sen’s Slope Estimator Test**

True slope in time series data is estimated by Sen’s procedure [46]. According to [47], Sen’s method is very robust against outliers. The magnitude of the trend is predicted by the Sen’s slope estimator ( $Q$ ).

$$(Q_i) = \frac{X_j - X_k}{j - k} \text{ for } i = 1, 2, \dots \dots \dots, N, \quad (8)$$

where,  $X_j$  and  $X_k$  are data values at times  $j$  and  $k$  ( $j > k$ ), respectively. The median of  $N$  values of  $Q_i$  is represented as Sen’s slope estimator.  $Q_{med} = Q_{(N+1)/2}$  if  $N$  is even. Positive value of  $Q$  indicates an increasing trend and a negative value shows a decreasing trend in time series.

**4. Results**

*4.1. Frequency and Spatial Distribution of Drought and Wet Conditions*

The spatial distribution of the PNPI drought and wet conditions across the province from 1970 to 2017 is shown in Figure 4. There is a variation in the PNPI drought index from year to year throughout the province where some of the years are drier and others are wetter. Severe to extreme droughts were recorded in 2015 and 2016. However, the 2016 severe drought is observed in the central and north-eastern region of the province. Moderate drought conditions were more prevalent in 1992, 2014 and 2017. Periods dominated by normal conditions are results of the occurrence of above normal

rainfall. The PNPI shows more years of weak drought to normal conditions for the entire length of rainfall record. The wettest conditions (i.e., periods of normal conditions) were prevalent in 1971, 1976–1978, 1987–1989, 1995–2000 and 2006. A detailed inspection of the spatial distribution of the PNPI revealed a spatial variation in rainfall across the province and that wet and dry conditions are not peculiar to one region. However, it is important to note that the eastern and western parts of the province are dominated by periods of normal conditions and weak droughts as compared to moderate and severe droughts.

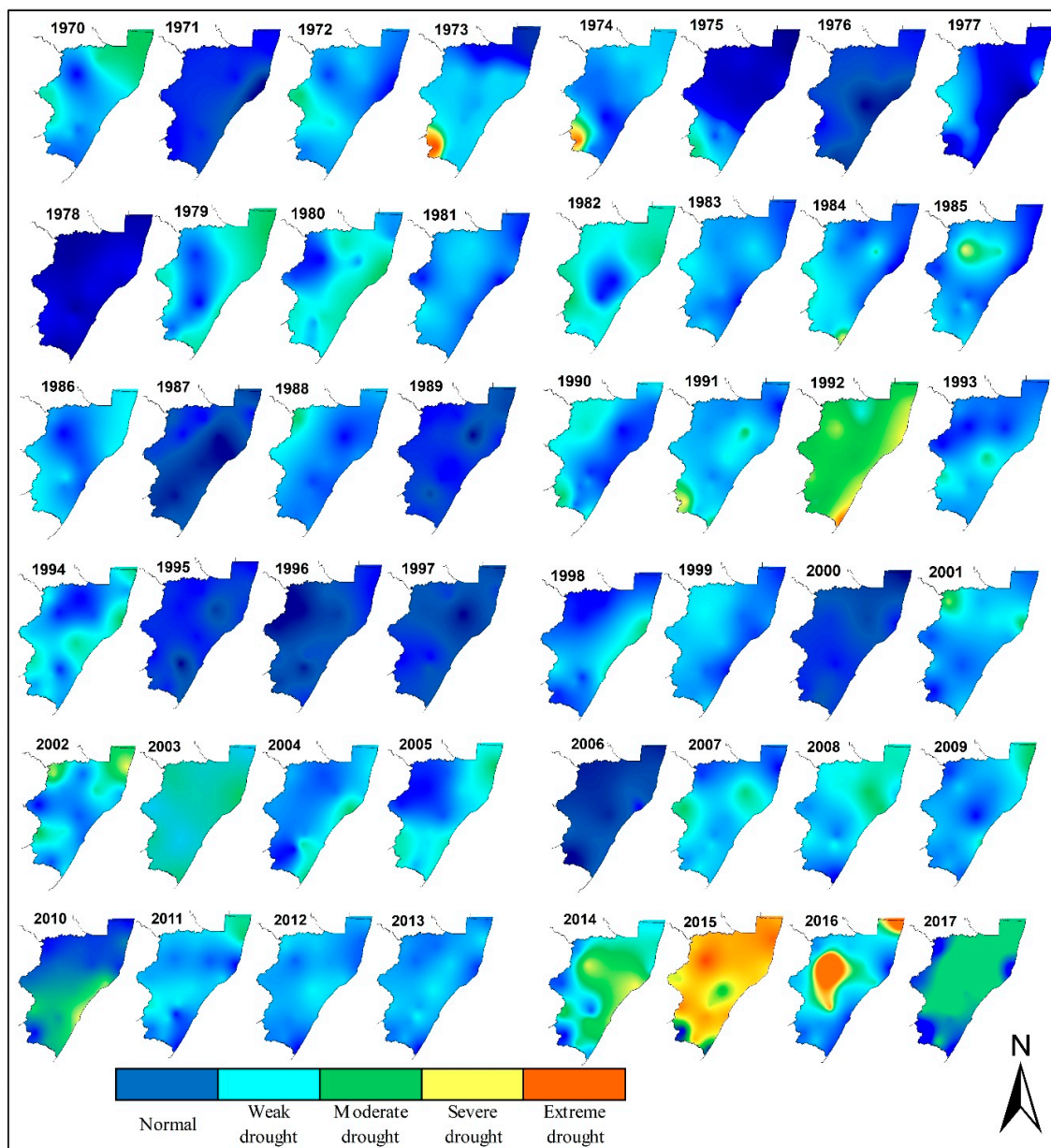


**Figure 4.** Spatiotemporal distribution of PNPI index across the KZN province.

The spatiotemporal distribution of RAI is presented in Figure 5. The RAI indices show more years with dry conditions as compared to wet conditions. The very dry to extremely dry conditions were prevalent in 1979–1980, 1992, 2002–2003, 2014 and 2015. Slightly dry to moderately dry conditions are widespread in 1970–1973, 1997, 1981, 1983, 1986, 1990–1991, 1993–1994, 2001, 2004, 2009–2011 and 2016. Similar drought conditions were reported by [16] in the Free State and North West provinces using the SPI and standardized precipitation evapotranspiration index (SPEI). Extremely wet to moderately wet

conditions were more prevalent in 1975–1976, 1978, 1987–1989, 1995–1997, 2000 and 2006. The driest and the wettest years were recorded in 1992 and 2014, and 1987, respectively. [48,49] made similar observations and indicated that 1992 and 1993 were the worst droughts in consecutive years and that 1987 was the wettest year attributed to cyclonic events. Through a visual inspection of the indices plot, it has been observed that very dry and extremely dry conditions have a cycle of 3–5 years and 10–12 years, respectively. The spatial distribution shows that regions in the northern parts of the KZN province recorded high magnitude of drought during a dry year. Similar observations were reported by [50] where the droughts of the early 1980s, 1990s and 2000s had the strongest expression over the eastern areas of South Africa. The drought indices do not indicate specific orographic effects on the distribution of wet and dry conditions, which is in line with the absence of any clear orographic effect in the rainfall–altitude plot of Figure 3. A comparison of the two indices indicates that the PNPI shows more wet conditions than the RAI.

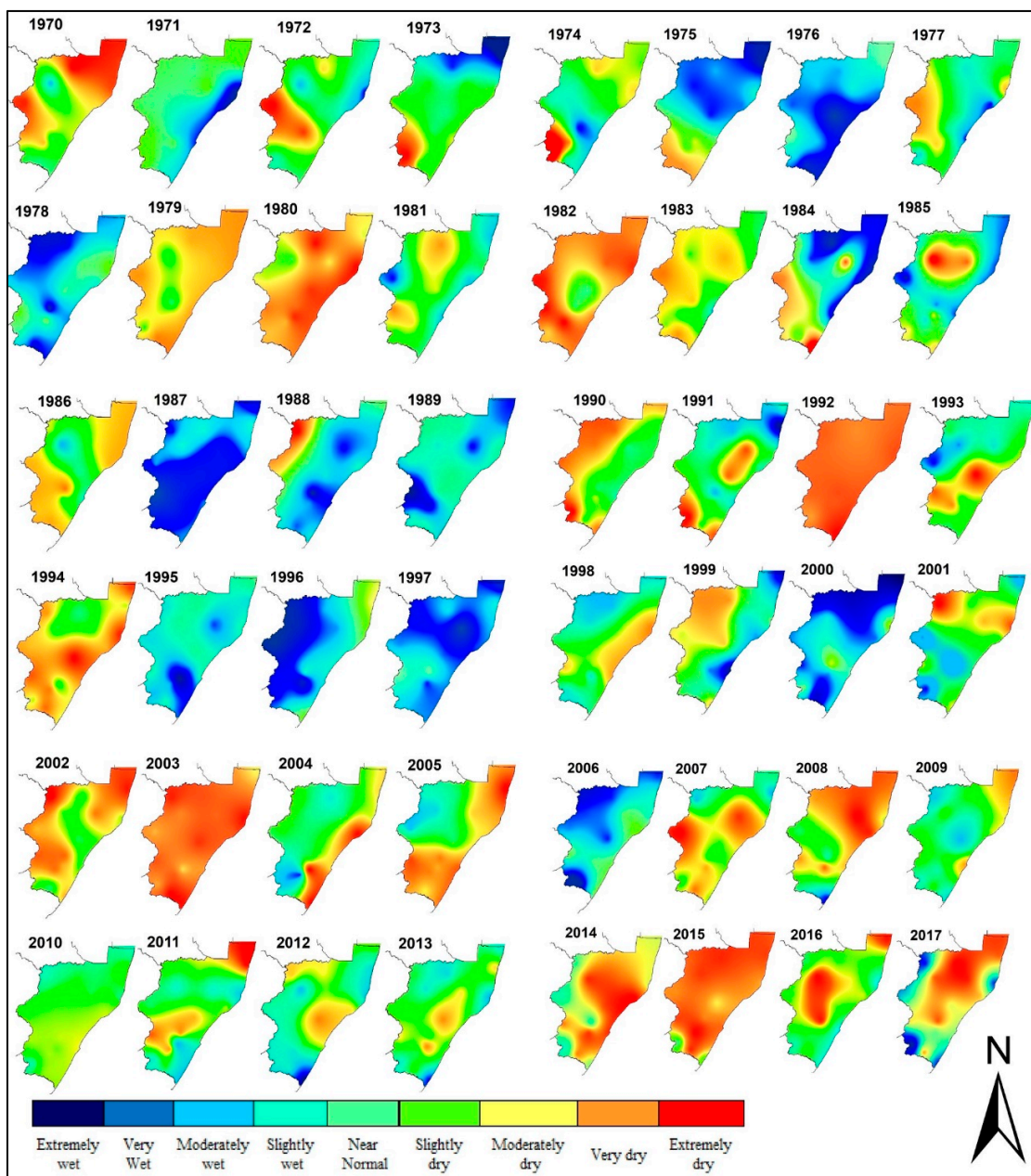


Figure 5. Spatiotemporal distribution of RAI index across the KZN province.

#### 4.2. Statistical Trend Analysis of Drought Indices

Statistical analyses of the PNPI and RAI indices using the Mann–Kendall trend test and Sen’s slope were undertaken at a 5% significance level and a 95% confidence interval in order to understand the change in the magnitude and intensity of drought indices for the entire record period i.e., 1970–2017. Table 4 shows summary results of the statistical analysis. Increasing and decreasing trends in both indices were detected at 4 (22%) and 14 (77%) of the rainfall gauging stations, respectively. The increasing trend in indices indicates an increase in wet conditions and a decreasing trend indicates a decrease in wet conditions (increase in drought severity). It was observed that significant trends exist within the data or indices and the null hypothesis ( $H_0$ ) has been rejected in favor of the alternative hypothesis ( $H_1$ ). The results of S value for the Mann–Kendal test are in agreement with the results of Sen’s slope for both RAI and PNPI. The stations that revealed increasing trends in wet conditions in the indices are located in the southern region (Margate and Franklin Pol stations) and in the north-western region (Newcastle and Bergville stations) of the province. The Ingwavuma-Manguzi station revealed the most decreasing trend whereas, Sani-Pass station revealed the least declining trend for both PNPI and RAI indices, in which case altitude appears to be important to proximity to the moisture source.

**Table 4.** Summary results of statistical analysis of drought indices (note the  $p$ -Values of stations that show statistically significant results are indicated in bold).

Rainfall Station	Altitude (m amsl)	S-Value	$p$ -Value	Sen’s Slope	
				RAI	PNPI
Ingwavuma-Manguzi	69	−131	<b>0.026</b>	−0.137	−1.617
Hlabisa- Mbazwana	55	−256	<b>0.023</b>	−0.056	−0.787
Hlobane	1294	−130	0.253	−0.028	−0.271
Newcastle	1241	17	0.814	0.005	0.056
Dundee	1256	−212	0.061	−0.046	−0.613
Mahlabathini	757	−156	0.169	−0.032	−0.409
St.Lucia Forest	44	0	0.993	$-9.8 \times 10^{-5}$	−0.001
Empangeni Magistrate	74	−336	<b>0.003</b>	−0.079	−1.135
Bergville	1145	78	<b>0.496</b>	0.021	0.194
Boscombe	1151	−286	<b>0.011</b>	−0.048	−0.484
Sani-Pass	2063	−20	0.867	−0.003	−0.038
Allerton Vet	711	−221	<b>0.049</b>	−0.051	−0.467
Richmond	864	−71	0.528	−0.017	−0.233
Durban	76	−288	<b>0.01</b>	−0.06	−0.708
SummerFord	1233	−20	0.867	−0.005	−0.046
Franklin Pol	1532	304	<b>0.007</b>	0.058	0.765
Glenora Farm	872	−134	0.239	−0.02	−0.193
Margate	127	123	0.07	0.078	0.879

The time series plots of PNPI and RAI indices along with Sen’s slopes are presented in Appendix A, respectively. The time series plots show variation in the drought indices from year-to-year throughout the record period. This in turn suggests that rainfall varied from year-to-year. The negative values of RAI represent the dry years, with different intensity. Tables 5 and 6 show descriptive statistics of the PNPI and RAI indices for the analyzed rainfall stations, respectively. Both indices show that 50%, 16% and 11% of rainfall stations have minimum values in 2015, 2014 and 1992, respectively. Whereas the maximum values are observed in 39%, 22% and 11% of the rainfall stations in 1987, 1996 and 2000, respectively. This is in agreement with the spatiotemporal changes presented in Section 4.1. Figure 6 shows the spatial distribution of Sen’s slope for PNPI and RAI across the province for the entire record period. It shows that the north-eastern region is characterized by the most significant decline in drought indices followed by eastern and central regions of the province. The western region of the province shows the least declining trend. The south-western and south-eastern regions revealed a positive slope indicating a decrease in drought occurrence and severity.

**Table 5.** Descriptive statistics of PNP index (%).

Rainfall Station	Minimum		Maximum		Mean	$\sigma$
Ingwavuma-Manguzi	52.94	(2015)	197.17	(2000)	100.0	33.8
Hlabisa- Mbazwana	37.29	(2015)	167.58	(1991)	100.0	32.2
Hlobane	53.57	(2015)	154.88	(1994)	100.0	21.7
Newcastle	54.99	(2002)	159.63	(1996)	100.0	26.4
Dundee	30.10	(2015)	161.67	(1996)	100.0	29.6
Mahlabathini	54.29	(2015)	181.81	(1987)	100.0	32.4
St.Lucia Forest	50.35	(1992)	170.15	(1984)	100.0	30.0
Empangeni Magistrate	37.70	(2014)	177.74	(1987)	100.0	33.6
Bergville	59.34	(2007)	157.23	(1996)	100.0	20.8
Boscombe	66.38	(2014)	167.39	(1987)	100.0	22.7
Sani-Pass	44.25	(2015)	144.54	(1987)	83.1	17.9
Allerton Vet	64.27	(2016)	159.05	(1987)	100.0	20.8
Richmond	49.43	(2015)	165.42	(1996)	99.5	24.4
Durban	48.21	(2014)	147.65	(1999)	100.0	26.1
SummerFord	53.25	(2015)	173.92	(1987)	100.0	21.6
Franklin Pol	28.81	(1974)	162.61	(1987)	100.6	29.1
Glenora Farm	55.16	(2015)	149.80	(2000)	100.0	20.5
Margate	39.74	(1992)	179.75	(2012)	100.0	30.2

**Table 6.** Descriptive statistics of RA index.

Rainfall Station	Minimum		Maximum		Mean	$\sigma$
Ingwavuma-Manguzi	-4.09	(2015)	7.75	(2000)	-0.10	2.79
Hlabisa- Mbazwana	-4.55	(2015)	4.45	(1991)	-0.09	2.22
Hlobane	-4.88	(2015)	5.51	(1994)	-0.04	2.23
Newcastle	-4.24	(2002)	5.74	(1996)	0.02	2.52
Dundee	-4.69	(2015)	5.08	(1996)	0.18	2.18
Mahlabathini	-3.81	(2015)	4.86	(1987)	-0.31	2.22
St.Lucia Forest	-3.91	(1992)	4.81	(1984)	-0.12	2.19
Empangeni Magistrate	-4.64	(2014)	4.67	(1987)	-0.20	2.22
Bergville	-4.24	(2007)	6.30	(1996)	0.05	2.23
Boscombe	-3.66	(2014)	5.92	(1987)	-0.18	2.18
Sani-Pass	-4.47	(2015)	14.10	(1987)	-0.88	2.87
Allerton Vet	-4.03	(2016)	5.71	(1987)	-0.13	2.16
Richmond	-5.06	(2015)	6.44	(1996)	-0.02	2.40
Durban	-4.14	(2014)	4.21	(1999)	0.09	2.19
SummerFord	-5.68	(2015)	6.99	(1987)	-0.22	2.27
Franklin Pol	-4.84	(1974)	5.21	(1987)	0.21	2.18
Glenora Farm	-5.09	(2015)	5.06	(2000)	-0.09	2.19
Margate	-5.42	(1992)	6.68	(2012)	-0.08	2.62

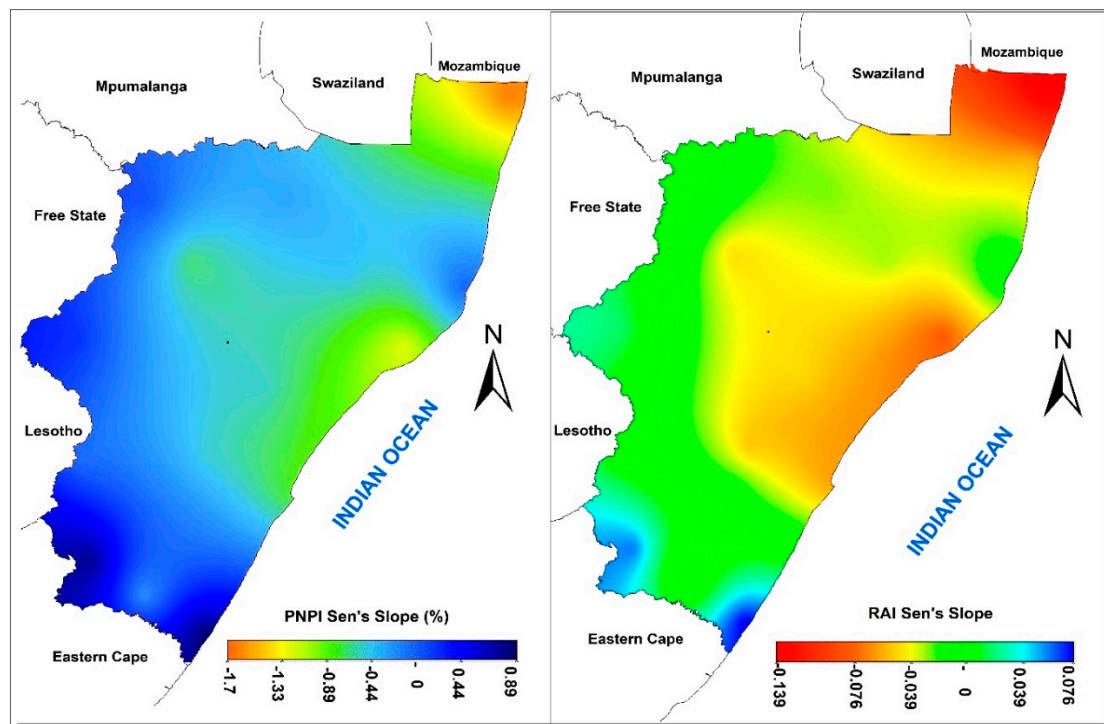


**Figure 6.** Spatial distribution of Sen's slope for (a) PNPI and (b) RAI for the period from 1970 to 2017.

## 5. Discussion

The spatial and temporal variation of rainfall in the province is evident as rainfall decreases from the coastal areas inland. However, rainfall increases again from the central areas towards the western part of the province along the Drakensberg mountain range due to what appears to be an orographic effect at least for the Sani-Pass rainfall station. The north-eastern areas generally receive high rainfall, while the northern areas around Hlobane and Dundee receive a low annual rainfall of between 720 mm and 860 mm. In the region along the eastern and south-eastern coast of the province, rainfall increases towards the south with Margate receiving the highest annual rainfall of 1380 mm.

Severe (very dry) to extreme droughts were mainly observed in 1992–1993 and 2015–2016. Whereas, wet to extremely wet years were 1987, 1996 and 2000. It has been observed that drought frequency has increased over the record period. According to [48], in 1992–1993 summer periods, the rainfall over south-east Africa and KZN was below average as a result of an offshore water vapor flux, low precipitable water and surface divergence. Severe (very dry) and extremely dry conditions have a cycle of 3–5 and 10–12 years, respectively.

Statistical analysis of drought indices revealed significant increasing and decreasing trends in both indices in 22% and 78% of the rainfall stations, respectively. This trend shows that 78% of the stations have recorded an increase in drought severity (i.e., decrease in wet conditions). The Ingwavuma-Manguzi rainfall station shows the highest decreasing trend ( $-0.137$  and  $-1.617$  for RAI and PNPI, respectively) indicating an increase in drought severity. Some stations that show increasing trends of the indices indicate an increase in wet conditions. The results of the Mann–Kendal trend test are in agreement with the results of Sen's slope for both RAI and PNPI. The descriptive statistics show that minimum values were recorded at 50%, 16% and 11% of stations in 2015, 2014 and 1992, respectively. Whereas maximum values are observed in 39%, 22% and 11% of the rainfall stations in 1987, 1996 and 2000, respectively. The overall spatial analysis of the drought indices showed that drought conditions are not peculiar to one region of the province and vary from year to year. This variation has been linked to ENSO and SST as the main drivers of interannual rainfall variability [9,13]. Studies [11,51] have shown that abnormally warm SST in the Indian Ocean are associated with intense

or reduced precipitation. In Southern Africa, drought periods are associated with El Niño events [52] and during drought periods the northern region of the province is mostly affected by severe drought conditions. The extremely wet conditions observed in the north-eastern region in 1984 and 2000 were associated with tropical cyclone Domoina [53,54] and tropical cyclone Eline [55], respectively. This is consistent with the tracks of tropical cyclones which mainly affect the north-eastern part of KZN, Mozambique and Swaziland [53,55]. There are no conspicuous orographic effects observed on the drought indices as both high and low altitude regions have experienced similar extreme drought conditions in the same year.

During the 2014–2015 hydrological year, the dam storage levels across the province were reduced to less than 50% due to the severe drought. Six of the large dams in the province, namely Albert Falls, Geodertrouw, Hazelmere, Klipfontein, Hluhluwe and Midmar were critically low during 2014–2016 [35] prompting water use restriction across the province. For instance, the Hazelmere dam storage level was less than 26% and the Hluhluwe dam was at 22% due to reduction of water inflow from 280 to 90 m<sup>3</sup>/hour, prompting a further increase of water use restrictions from 15% to 50%.

Comparative analyses of the two indices indicate that PNPI shows more years of normal conditions whereas RAI shows more years of dry conditions. Additionally, RAI gives more details on dry and wet conditions than the PNPI. This is because of the fact that PNPI does not account for wet to extremely wet years since it considers all values greater than 80% as normal conditions. Thus, RAI can be effectively used in Southern Africa to map meteorological drought conditions.

## 6. Conclusions

Analyses of meteorological drought and wet condition across the KZN province has been successfully undertaken by applying PNPI and RAI drought indices on annual rainfall data that spans from 1970 to 2017. The results show that both drought frequency and severity have increased in recent years. The most extreme dry periods were in 1992–1993 and 2015–2016. The extreme wet years were 1984 and 2000 which are related to tropical cyclones. The number of extreme dry years are much higher than the number of wet years over the studied period. The drought indices show that severe (very dry) drought have a cycle of 3–5 years whereas extreme drought conditions have a 10–12 year cycle. However, this study shows that extreme drought conditions have become more frequent in recent decades. The identified extreme drought and wet conditions are mainly the result of changes taking place in the moisture source region caused by regional to global drivers such as ENSO and SST. Although both indices identified and characterized drought and wet conditions, comparative analyses of the results of PNPI and RAI generating dry conditions indicate that the RAI identified extreme and severe drought conditions more clearly and robustly than PNPI.

The identified drought conditions have, obviously, brought about a decrease in rainfall across the province, significantly impacting the water resources and its availability for domestic, agricultural and other socio-economic activities. The increasing frequency and severity of the dry spells means that both surface and groundwater resources in the province have been constantly declining over the past decade. Therefore, a proactive science-based policy involving all stakeholders is essential for drought management and building long-term resilience.

**Author Contributions:** Conceptualization, M.S.N. and M.D.; methodology, M.S.N. and M.D.; validation, M.S.N. and M.D.; formal analysis, M.S.N. and M.D.; investigation, M.S.N. and M.D.; data curation, M.S.N.; writing—original draft preparation, M.S.N. and M.D.; writing—review and editing, M.D.; visualization, M.S.N.; supervision, M.D.; project administration, M.D. All authors have read and agree to the published version of the manuscript.

**Funding:** This research received no external funding.

**Acknowledgments:** The South African Weather Service is acknowledged for supplying the rainfall data used in this study.

**Conflicts of Interest:** Authors declare no conflict of interest.

Appendix A Appendix

Appendix A.1

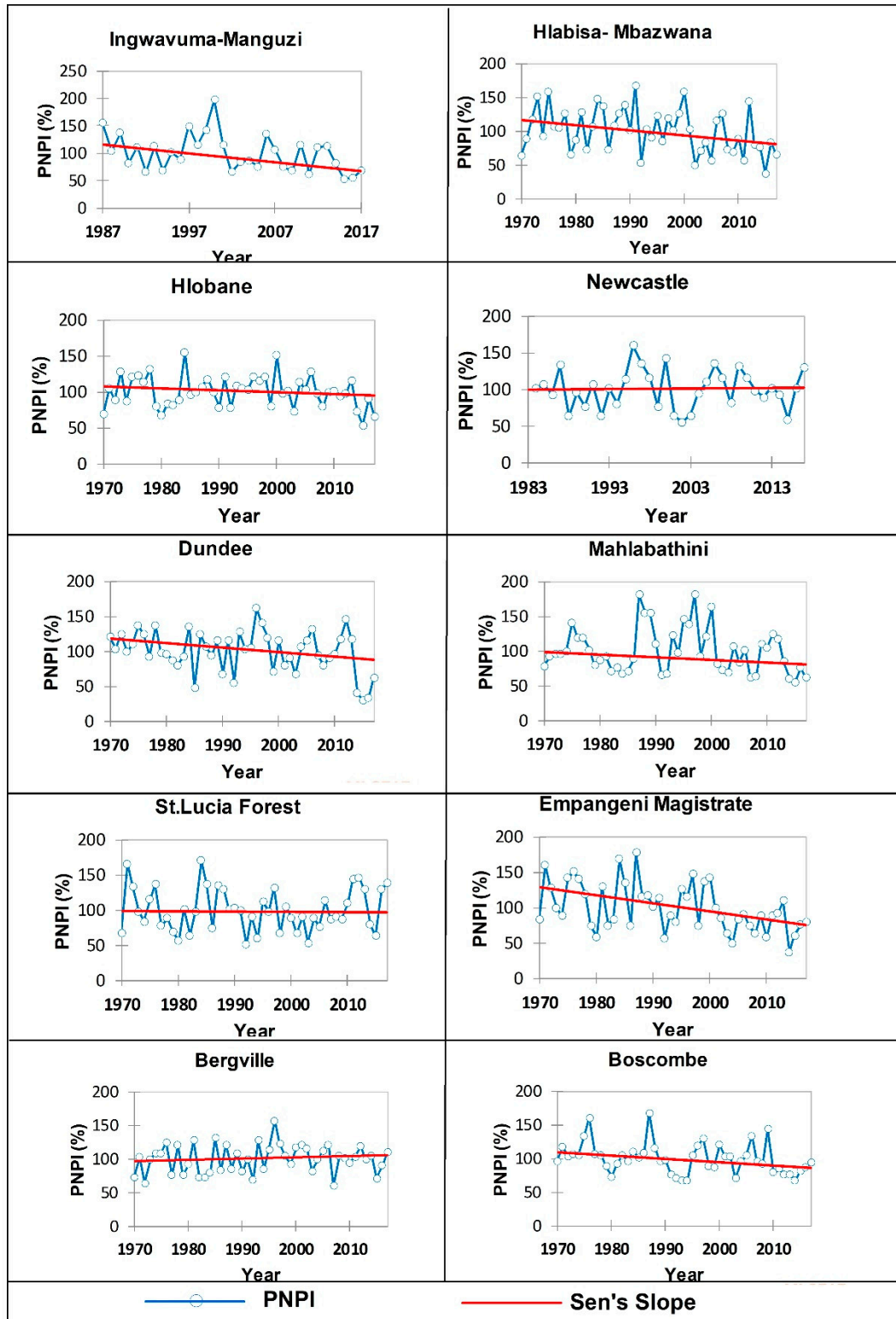


Figure A1. Cont.

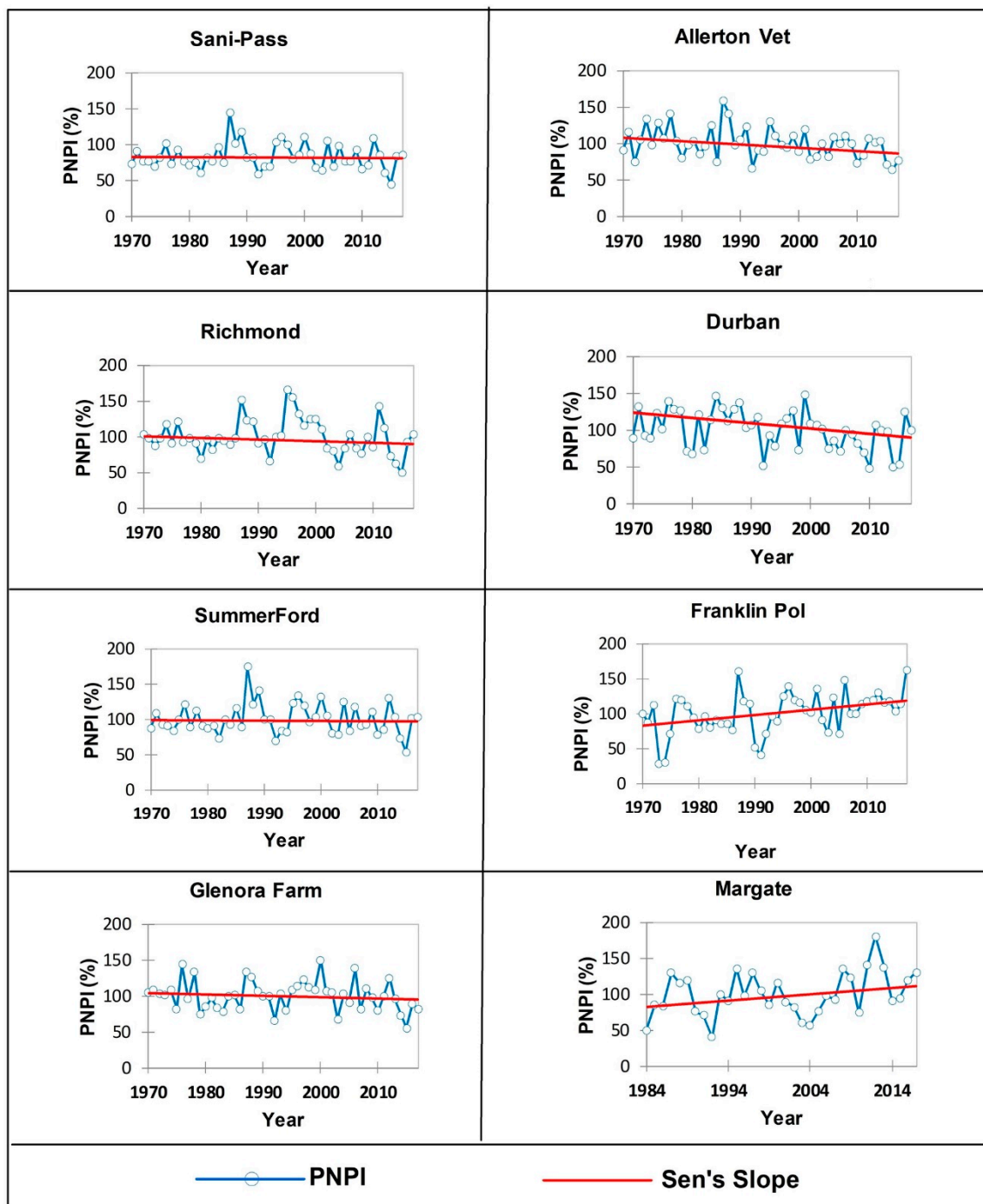


Figure A1. Time Series Plots of *PNPI* Drought indices and Sen's Slope for the Various Rainfall Stations.

Appendix A.2

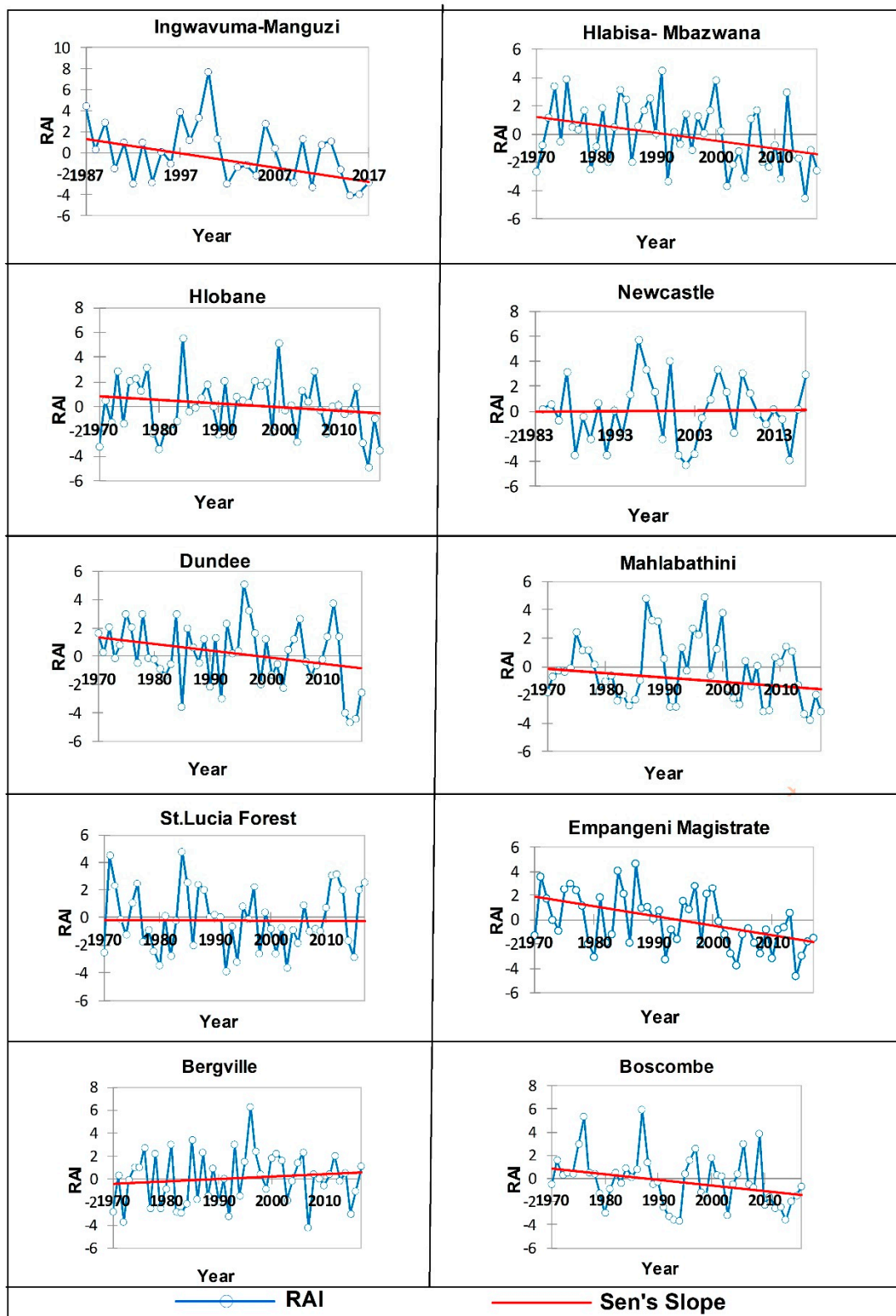


Figure A2. Cont.

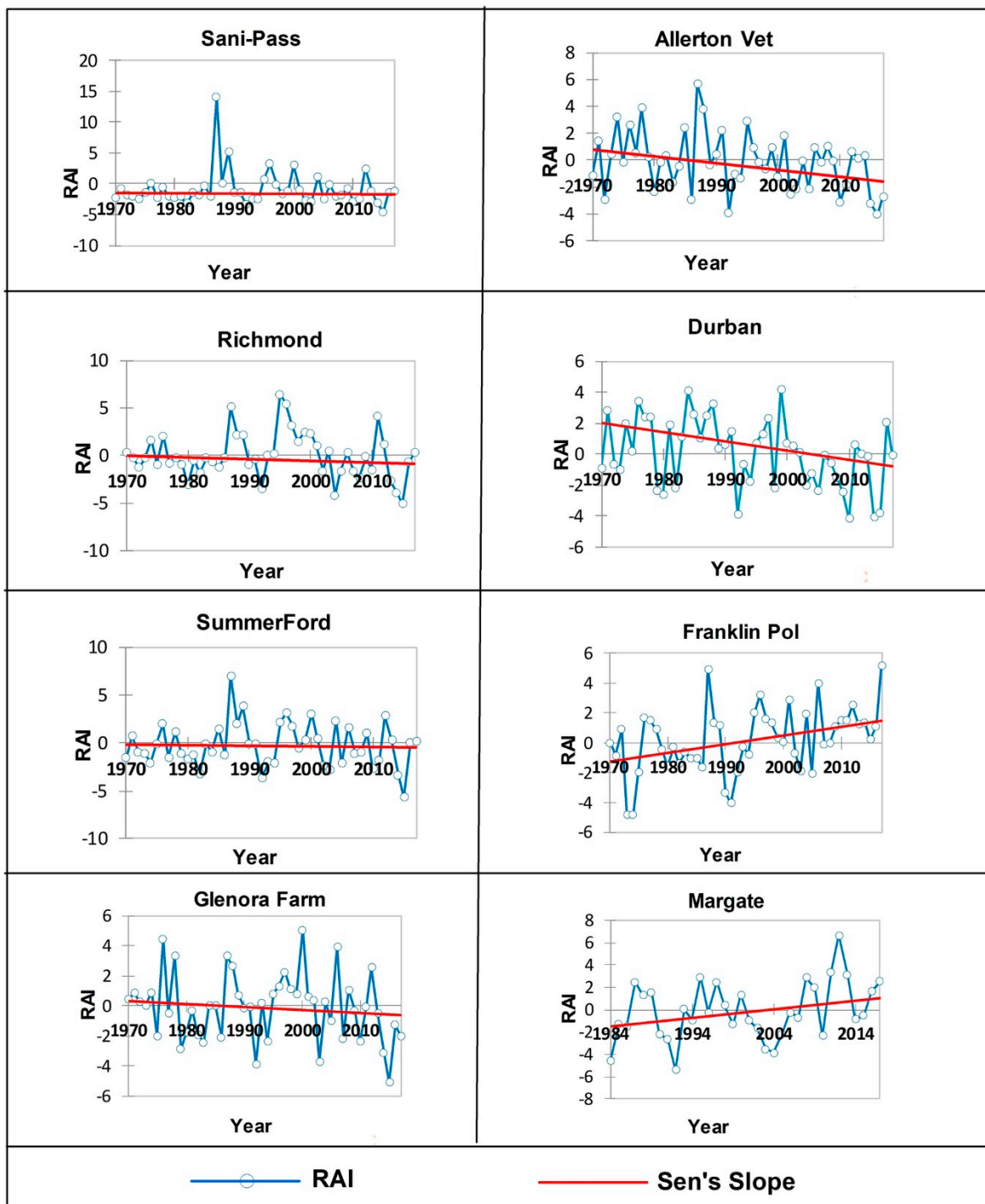


Figure A2. Time Series Plots of RAI Drought indices and Sen's Slopes for Various Rainfall Stations.

References

1. Department of Water Affairs and Forestry. *National Groundwater Strategy*; Department of Water Affairs and Forestry: Pretoria, South Africa, 2010.
2. World Meteorological Organization (WMO). *International Meteorological Vocabulary*, 2nd ed.; World Meteorological Organization: Geneva, Switzerland, 1992.

3. Department of Water and Sanitation. *Drought Status Report: November 2015*; Department of Water and Sanitation: Pretoria, South Africa, 2015.
4. Hove, L.; Kambanje, C. Lessons from the El Niño-induced 2015/16 drought in the Southern Africa region. *Curr. Dir. Water Scarcity Res.* **2019**, *33*–54. [[CrossRef](#)]
5. Tyson, P.D.; Preston-Whyte, R.A. *The Weather and Climate of Southern Africa*, 2nd ed.; Oxford University Press Southern Africa: Cape Town, South Africa, 2000; pp. 228–236.
6. Nicholson, S.E.; Leposo, D.; Grist, J. The relationship between El Niño and drought over Botswana. *J. Clim.* **2001**, *14*, 323–335. [[CrossRef](#)]
7. Rouault, M.; Richard, Y. Intensity and spatial extension of drought in South Africa at different time scales. *Water Sa* **2003**, *29*, 489–500. [[CrossRef](#)]
8. Ratnam, J.V.; Behera, S.K.; Masumoto, Y.; Yamagata, T. Remote effects of El Niño and Modoki events on the Austral Summer Precipitation of Southern Africa. *J. Climatol.* **2014**, *27*, 3802–3815. [[CrossRef](#)]
9. Dieppois, B.; Rouault, M.; New, M. The impact of ENSO on Southern African rainfall in CMIP5 ocean atmosphere coupled climate models. *Clim. Dyn.* **2015**, *45*, 2425–2442. [[CrossRef](#)]
10. Walker, N.D.; Lindesay, J.A. Preliminary observations of oceanic influences on the February–March 1988 floods in central South Africa. *S. Afr. J. Sci.* **1989**, *85*, 164–169.
11. Reason, C.J.C.; Mulenga, H. Relationships between South African rainfall and SST anomalies in the south west Indian Ocean. *Int. J. Climatol.* **1999**, *19*, 1651–1673. [[CrossRef](#)]
12. Camberlin, P.; Diop, M. Inter-relationships between groundnut yield in Senegal, interannual rainfall variability and sea-surface temperatures. *Theor. Appl. Climatol.* **1999**, *63*, 163–181. [[CrossRef](#)]
13. Fauchereau, N.; Trzaska, S.; Richard, Y.; Roucou, P.; Camberlin, P. Sea-surface temperature co-variability in the Southern Atlantic and Indian Oceans and its connections with the atmospheric circulation in the Southern Hemisphere. *Int. J. Climatol.* **2003**, *23*, 663–677. [[CrossRef](#)]
14. Nicholson, S.E.; Kim, J. The relationship of the El Niño–Southern Oscillation to African rainfall. *Int. J. Climatol.* **1997**, *17*, 117–135. [[CrossRef](#)]
15. Hewitson, B.C.; Tenant, W.; Walawege, R. *Atmospheric moisture transport and sources for South Africa*; WRC Report, No. 1024/1/04; 2004; WRC: Pretoria, South Africa.
16. Botai, C.M.; Botai, J.O.; Dlamini, L.C.; Zwane, N.S.; Phaduli, E. Characteristics of Droughts in South Africa: A Case Study of Free State and North West Provinces. *Water* **2017**, *8*, 439. [[CrossRef](#)]
17. Keyantash, J.; Dracup, J.A. The Quantification of Drought: An Evaluation of Drought Indices. *Bull. Am. Meteorol. Soc.* **2000**, *83*, 1167–1180. [[CrossRef](#)]
18. Morid, S.; Smakhtin, V.; Moghaddasi, M. Comparison of seven meteorological indices for drought monitoring in Iran. *Int. J. Climatol.* **2006**, *26*, 971–985. [[CrossRef](#)]
19. Salehnia, N.; Alizadeh, A.; Sanaeinejad, H.; Bannayan, M.; Zarrin, A.; Hoogenboom, G. Estimation of meteorological drought indices based on AgMERRA precipitation data and station-observed precipitation data. *J. Arid Land* **2017**, *9*, 797–809. [[CrossRef](#)]
20. Afzalia, A.; Keshtkarb, H.; Pakzada, S.; Moazamia, N.; Azizabadi Farahania, E.A.; Golpaygania, A.; Khosrojerdia, E.; Yousefia, Z.; Taghi Naghiloua, M. Spatio-Temporal Analysis of Drought Severity Using Drought Indices and Deterministic and Geostatistical Methods (Case Study: Zayandehroud River Basin). *Deserts* **2016**, *21*, 165–172.
21. Wilhite, D.A.; Glantz, M. Understanding the drought Phenomenon: The Role of Definitions. *Water Int.* **1985**, *10*, 111–112. [[CrossRef](#)]
22. Wilhite, D. *Drought: A Global Assessment*; Routledge: New York, NY, USA, 2000; p. 752.
23. World Meteorological Organization. *Drought Monitoring and Early Warning: Concepts, Progress and Future Challenges*; WMO-No. 1006; World Meteorological Organization: Geneva, Switzerland, 2006.
24. Asefjah, B.F.; Fanian, Z.; Feizi, A.; Abolhasani, H.; Paktinat, M.; Naghilou, A.; Molaei Atani, M.; Asadollahi, M.; Babakhani, A.; Kouroshnia, F.; et al. Drought monitoring by using several meteorological drought indices (Case study: Salt Lake Basin of Iran). *Desert* **2014**, *19*, 155–165.
25. Palmer, W.C. *Meteorological Drought*; Research Paper, No. 45; U.S. Weather Bureau: Washington, DC, USA, 1965.

26. Shafer, B.A.; Dezman, L.E. Development of a Surface Water Supply Index (SWSI) to assess the severity of drought conditions in snowpack runoff areas. In Proceedings of the Western Snow Conference, Colorado State University, Fort Collins, CO, USA, 19–23 April 1982; pp. 164–175.
27. McKee, T.B.; Doesken, N.J.; Kleist, J. The relationship of drought frequency and duration to time steps. Preprints. In Proceedings of the 8th Conference on Applied Climatology, Anaheim, CA, USA, 22 January 1993; pp. 179–184.
28. Willeke, G.; Hosking, J.R.M.; Wallis, J.R.; Guttman, N.B. *The National Drought Atlas*; Institute for Water Resources Report 94-NDS-4; U.S. Army Corps of Engineers: San Francisco, CA, USA, 1994.
29. Van Rooy, M.P. A rainfall anomaly index independent of time and space. *Notos* **1965**, *14*, 43–48.
30. Meyer, S.J.; Hubbard, K.G.; Wilhite, D.A. A crop-specific drought index for corn. Model development and validation. *Agron. J.* **1993**, *85*, 388–395. [[CrossRef](#)]
31. Barua, S.; Ng, A.W.M.; Perera, B.J.C. Comparative Evaluation of Drought Indexes: A Case Study on the Yarra River Catchment in Australia. *J. Water Resour. Plan. Manag.* **2011**, *137*, 215–226. [[CrossRef](#)]
32. Sneyer, R. *On the Statistical Analysis of Series of Observations*; Technical Note, no. 143, WMO No. 415; World Meteorological Organization: Geneva, Switzerland, 1990.
33. Subash, N.; Gangwar, B. Statistical analysis of Indian rainfall and rice productivity anomalies over the last decades. *Int. J. Climatol.* **2013**, *34*, 2378–2392. [[CrossRef](#)]
34. StatsSA. *Mid-Year Population Estimates: Statistics South Africa. P0302*; Statistics South Africa: Pretoria, South Africa, 2016; 17p.
35. Department of Water and Sanitation. *Digital Elevation Model*; Department of Water and Sanitation: Durban, South Africa, 2016.
36. Cook, C.; Reason, C.J.C.; Hewitson, B.C. West and dry spells within particularly wet and dry summers in the South African summer rainfall region. *Clim. Res.* **2004**, *26*, 17–31. [[CrossRef](#)]
37. Fetter, C.W. *Applied Hydrogeology*, 4th ed.; Prentice-Hall, Inc.: Upper Saddle River, NJ, USA, 2001; 589p.
38. Singh, V.P. *Elementary Hydrology*; Prentice Hall of India: New Delhi, India, 1994; 973p.
39. Ostad-Ali-Askari, K.; Eslamian, S.; Singh, V.P.; Dalezios, N.R.; Ghane, M.; Yihdego, Y.; Motouq, M. A review of drought index. *Int. J. Constr. Res. Civ. Eng.* **2017**, *3*, 48–66.
40. Javan, K.; Azzizadeh, M.R.; Yousefi, S. An Investigation and Assessment of meteorological drought in Lake Urma Basin using drought indices and probabilistic methods. *Nat. Environ. Chang.* **2016**, *2*, 153–164.
41. Mann, H.B. Non-parametric test against trend. *Econometrica* **1945**, *13*, 245–259. [[CrossRef](#)]
42. Kendall, M.G. *Rank Correlation Methods*; Charles Griffin: London, UK, 1975.
43. Wilks, D.S. Hypothesis Testing. In *Statistical Methods in the Atmospheric Sciences*; Academic Press: New York, NY, USA, 1995; pp. 160–176.
44. Yue, S.; Pilon, P.; Phinney, B.; Cavadias, G. The influence of autocorrelation on the ability to detect trend in hydrological series. *Hydrol. Process.* **2002**, *16*, 1807–1829. [[CrossRef](#)]
45. Luo, Y.; Liu, S.; Fu, S.; Liu, J.; Wang, G.; Zhou, G. Trends of precipitation in Beijiang River Basin, Guangdong province, China. *Hydrol. Process.* **2008**, *22*, 2377–2386. [[CrossRef](#)]
46. Sen, P.K. Estimates of the regression coefficient based on Kendall's tau. *J. Am. Stat. Assoc.* **1968**, *63*, 1379–1389. [[CrossRef](#)]
47. Hirsch, R.M.; Slack, J.R.; Smith, R.A. Techniques of trend analysis for monthly water quality data. *Water Resour. Res.* **1982**, *18*, 107–121. [[CrossRef](#)]
48. Dube, L.T.; Jury, M.R. Meteorological structure of the 1992/93 drought over eastern South Africa from ECMWF and satellite OLR analyses. *S. Afr. Geogr. J.* **2002**, *84*, 170–181. [[CrossRef](#)]
49. Terry, A.K. The impact of the 2015-16 El Nino drought on the irrigated home gardens of the Komati downstream development project, Swaziland. *S. Afr. Geogr. J.* **2019**. [[CrossRef](#)]
50. Malherbe, J.; Dieppois, B.; Maluleke, P.; Van Staden, M.; Pillay, D.L. South African droughts and decadal variability. *Nat. Hazards* **2016**, *80*, 657–681. [[CrossRef](#)]
51. Reason, C.J.C. Sensitivity of the southern African circulation to dipole sea-surface-temperature patterns in the south Indian Ocean. *Int. J. Climatol.* **2002**, *22*, 377–393. [[CrossRef](#)]
52. Lakhraj-Govender, R.; Grab, S.W. Assessing the impact of El Niño-Southern Oscillation on South African temperatures during austral summer. *Int. J. Climatol.* **2018**. [[CrossRef](#)]
53. Jury, M.R.; Pathack, B.; Wang, B.; Powell, M.; Raholita, N. A destructive Tropical cyclone season in the SW Indian Ocean: January–February 1984. *S. Afr. Geogr. J.* **1993**, *75*, 53–59. [[CrossRef](#)]

54. Matondo, J.I.; Msibi, K.M. Estimation of the impact of climate change on hydrology and water resources in Swaziland. *Water Int.* **2001**, *26*, 425–434. [[CrossRef](#)]
55. Reason, C.J.C.; Keibel, A. Tropical cyclone Eline and its usual penetration and impacts over the South African mainland. *Am. Meteorol. Soc.* **2004**, *19*, 789–805.



© 2020 by the authors. Licensee MDPI, Basel, Switzerland. This article is an open access article distributed under the terms and conditions of the Creative Commons Attribution (CC BY) license (<http://creativecommons.org/licenses/by/4.0/>).